

# White matter microstructure changes following working-memory training in survivors of neonatal critical illness: a Randomized Controlled Trial

Raisa Schiller,  
Hanneke IJsselstijn,  
Marlous J. Madderom,  
Joost van Rosmalen,  
Arno F.J. van Heijst,  
Marion Smits,  
Frank Verhulst,  
Dick Tibboel,  
Tonya White

*Submitted*

## ABSTRACT

**Objective** To test the effect of Cogmed Working-Memory Training (CWMT) on white matter microstructure following neonatal ECMO and/or CDH.

**Design** A nationwide randomized controlled trial assessing white matter microstructure immediately post-CWMT (T1) and its association with neuropsychological outcome immediately and one year (T2) post-CWMT, conducted between October 2014-June 2017. Researchers involved in the follow-up assessments were blinded to group allocation.

**Setting** Erasmus MC-Sophia Children's Hospital, Rotterdam and Radboud University Medical Center, Nijmegen, the Netherlands.

**Patients** Eligible participants were neonatal ECMO and/or CDH survivors (8-12 years) with an IQ  $\geq 80$  and a z-score  $\leq -1.5$  on at least one (working)memory test at first assessment.

**Interventions** CWMT, comprising 25 sessions of 45 minutes for five consecutive weeks at home.

**Measurements and Main Results** Participants were randomized to CWMT ( $n = 14$ ) or non-training ( $n = 20$ ). Global fractional anisotropy (FA) increased significantly in the CWMT group compared to the non-training group (estimated coefficient = .007,  $p = .015$ ). Increased FA (estimated coefficient = .009,  $p = .033$ ) and decreased mean diffusivity (estimated coefficient = -.010,  $p = .018$ ) were found in the left superior longitudinal fasciculus in the CWMT group compared to the non-training group at T1. Children in the CWMT who improved with at least 1 SD on verbal working-memory from T0 to T1 had significantly higher FA in the left SLF at T1 ( $n = 6$ ; FA left SLF at T1 =  $.408 \pm .01$ ) compared to children that did not show this improvement after CWMT ( $n = 6$ ; FA left SLF at T1 =  $.384 \pm .02$ ),  $F(1,12) = 6.22$ ,  $p = .041$ ,  $h_p^2 = .47$ . No other structure-function relationships were found after CWMT.

**Conclusions** White matter microstructure is affected by CWMT in school-age survivors of neonatal ECMO and/or CDH. Our findings demonstrate that white matter microstructure and associated cognitive outcomes are malleable in these children.

**TrialRegistration** NTR4571: <http://www.trialregister.nl/trialreg/admin/rctview.asp?TC=4571>.

## INTRODUCTION

Survivors of neonatal extracorporeal membrane oxygenation (ECMO) and/or congenital diaphragmatic hernia (CDH) are at increased risk of specific attention and memory deficits that begin during the school-age years and extend into adolescence.<sup>1,2</sup> These deficits have been found to be specifically associated with global white matter microstructure alterations and with specific alterations in limbic regions of the brain, namely the hippocampus, cingulum and parahippocampal part of the cingulum.<sup>3-5</sup> Using a single-blind randomized controlled trial, we recently found that school-age survivors of neonatal ECMO and/or CDH trained with Cogmed working-memory training (CWMT<sup>6</sup>) showed significant improvements in verbal and visuospatial working-memory immediately post-intervention compared to untrained controls (chapter 7). However, this improvement was not maintained at the one year post-intervention assessment. Interestingly however, improvements in visuospatial memory delayed recall were found to persist one year post-intervention compared to controls (chapter 7). Given the fact that more than 50% of these survivors have visuospatial memory deficits later in life<sup>1</sup> and considering the importance of memory for both academic performance and participation in society, this is a promising finding.

Several studies in adults have shown plasticity in white matter microstructure immediately following working-memory training.<sup>7,8</sup> In particular, the superior longitudinal fasciculus (SLF) has shown plastic changes following working-memory training, likely because it connects parietal and frontal cortical regions, which have been shown to be important for working-memory.<sup>9</sup> Given the increased plasticity of a child's brain compared to that of an adult<sup>10</sup>, white matter microstructure changes may be more widespread following CWMT in children compared to adults. However, this has remained unstudied until now.

The aim of this study was to investigate the neurobiological plasticity following CWMT using diffusion tensor imaging (DTI) in school-age survivors of neonatal ECMO and/or CDH that were part of a nationwide single-blind randomized controlled trial. We hypothesized that white matter microstructure, and in particular the SLF, would change following CWMT. Furthermore, we assessed whether if there were changes in white matter microstructure, these were associated with the cognitive improvements observed following CWMT (chapter 7).

## METHODS

### Design and population

This nationwide randomized controlled trial, conducted between October 2014 and June 2017, compared CWMT to no training in school-age neonatal ECMO and/or CDH survivors (NTR4571). Inclusion criteria for the trial were: school-age children (8-12 years) treated with ECMO or treated for CDH without ECMO in the first weeks of life at the Erasmus MC-Sophia Children's Hospital in Rotterdam or the Radboud University Medical Center in Nijmegen (the Netherlands), IQ  $\geq 80$  and memory impairment ( $z$ -score  $\leq -1.5$  on one or more memory tests<sup>11</sup>). Exclusion criteria were: usage of psychopharmaceutic drugs (e.g. methylphenidate) and/or genetic syndromes that are known to affect neuropsychological functioning. Eligible children were randomized into either the CWMT group or the non-training group by an independent researcher not involved with the assessment of the children (please refer to Figure 1 for the trial outline). The MRI exam and neuropsychological assessments were performed by researchers blinded to group allocation.

Ethical approval was granted by the Erasmus MC Medical Ethical Review Board (MEC-2014-001). All families received an application package with written informed consent for the parents and children  $\geq 12$  years of age that was discussed with the family and filled out before participating in the trial. The complete trial methods are described elsewhere (chapter 7).

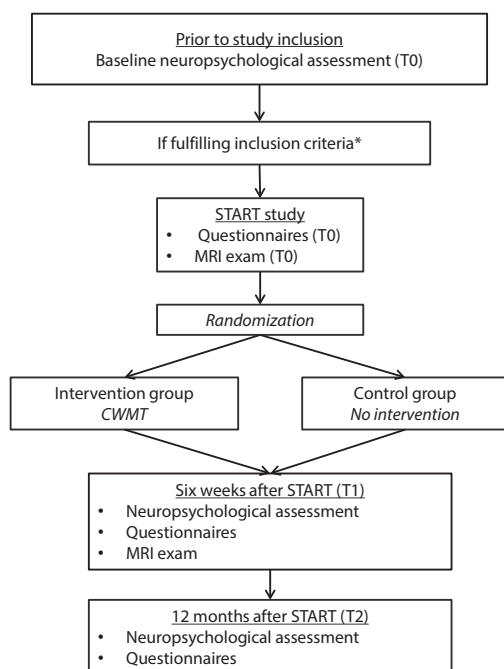


**Figure 1.** Trial outline

For short descriptions of the tests and questionnaires used, please refer to Supplemental File 1. For description of the MR methods please refer to Supplemental File 2. \*IQ  $> 80$  and a  $z$ -score  $\leq -1.5$ (20) on one or more memory tests. Abbreviations: CWMT, Cogmed Working-Memory Training.

## Intervention

Children in the CWMT group completed the CWMT<sup>RM</sup> version for children from the ages 7 to 17 years. Children trained at home for 45 minutes a day, five days a week, for five consecutive weeks, as recommended in the manufacturer's instructions.<sup>6</sup> The level of the tasks adapted automatically to ensure that the child was continuously performing at the maximum of his or her ability. As part of the program, each child was supervised by a certified CWMT coach, who provided support to the family and feedback on the training results once a week over the phone and by e-mail. The CWMT coach was able to closely monitor the child's performance via online access.

Children in the non-training group did not receive any training.

## Outcome measures

After the standardized, neuropsychological assessment at baseline to determine eligibility, eligible participants underwent an MRI exam (T0). After six weeks, the MRI exam was repeated in all participants (T1). At the same time, the neuropsychological assessment was repeated, and again after one year following the baseline measurement (T2, neuropsychological assessment only). The neuropsychological outcomes are described elsewhere (chapter 7; please refer to Supplemental File 1 for brief descriptions of all cognitive tests).

All children first underwent a mock scanning session to become familiarized with the MRI-scanner environment.<sup>12</sup> MRI data were acquired on a 3 Tesla GE MR-750 system using an 8-channel head coil (General Electric, Milwaukee, WI). A full description of the sequences and scanning protocol is provided in Supplemental File 2. After DTI image preprocessing, voxel-wise scalar maps of fractional anisotropy (FA) and mean diffusivity (MD) were computed. FA provides a rotationally invariant measure of diffusion, with 0 being completely isotropic (equal in all directions) and 1 being completely anisotropic (diffusion along only one axis). MD is the rate of diffusion of water (hydrogen) averaged in all directions. The FSL plugin 'AutoPtx' for fully automated probabilistic fiber tractography was used to create subject-specific, probabilistic representations of multiple white matter bundles.<sup>13</sup> Automated<sup>14</sup> and visual inspection of the neuroimaging data resulted in 61 DTI datasets (87%) with usable image quality. All scans were reviewed by a certified neuroradiologist (M.S.), blinded for medical history and outcome.

## Statistical analysis

Clinical and demographic characteristics and neuropsychological outcome at baseline were compared between groups using independent samples t-tests and ANOVA (normally distributed variables), Mann-Whitney U or Fisher's exact tests (non-normally distributed continuous or categorical variables, respectively).

First, we assessed whether white matter microstructure changed as a result of CWMT. Our primary aim was to assess changes in the SLF as it is involved in working-memory and has previously been shown to be affected by CWMT.<sup>9</sup> Linear mixed models were estimated to assess whether white matter microstructure changed in the CWMT group compared to the non-training group at T1. This method accounts for within-subject correlations and allows for missing values in the dependent variable. Outcome at baseline was constrained to be equal. The brain diffusion measures were included as dependent variables, and group and time-point as well as the group by time-point interaction term were included as independent variables. Results of the linear mixed models were summarized using the estimated marginal means (the predicted values of the dependent variable adjusted for the effects of the independent variables) of the group by time-point interaction.

Second, we analyzed changes in global FA and global MD following CWMT using linear mixed models. Described by our group in more detail elsewhere<sup>5</sup>, global white matter microstructure was calculated using a weighted (by tract volume) average score of FA/MD of the association and limbic system white matter tracts (uncinate, inferior fronto-occipital fasciculus, SLF, inferior longitudinal fasciculus, cingulum bundle and parahippocampal part of cingulum) (Equation 1), known to be involved with cognitive functioning in children<sup>14,15</sup>:

Equation 1:

$$\text{Global FA} = \frac{\sum_{i=1}^n \text{FAtract}_i \text{Voltract}_i}{\sum_{i=1}^n \text{Voltract}_i}$$

where  $i$  denotes the tract,  $\text{Vol}$  denotes the volume of the tract, and  $n$  is the number of tracts. The same formula was used for global MD, replacing FA for each tract with the MD measure.

If global FA or global MD changed significantly following CWMT, additional analyses were performed with the individual white matter tracts. The same setup of linear mixed models were used to now assess whether white matter microstructure in the individual tracts (independent variables) changed in the CWMT group compared to the non-training group at T1. Brain structures were analyzed in the left and right hemispheres separately as laterality differences have been shown in the organization of working-memory and specific cognitive functions.<sup>16</sup> In all linear mixed models, we adjusted for age at T1 and gender.<sup>17</sup> For the additional analyses on group differences in the individual white matter tracts, the False Discovery Rate (FDR)<sup>18</sup> correction was applied to account for multiple testing. These results were considered statistically significant at the FDR-corrected  $p < .05$ .

Our previous findings showed that children trained with CWMT improved significantly on verbal working-memory, visuospatial working-memory and visuospatial memory

delayed recall compared to non-trained children (chapter 7). For our second aim, we therefore assessed whether changes in white matter microstructure following CWMT (if any) were associated with the cognitive improvements in the CWMT group using univariate linear regression models. The dependent variable was the brain parameter at T1 in the CWMT group and the independent variable was the cognitive outcome measure, dichotomized to: improved ( $>1$  SD improvement from T0 to T1) versus not improved ( $<1$  SD improvement from T0 to T1). In these analyses, we adjusted for FA/MD at baseline, age at T1 and gender. Neuropsychological test scores were converted to z-scores (individual score minus the population mean divided by the population SD). Scores were inverted where appropriate so that a higher score always equated with better performance.

Statistical analyses were performed using SPSS 21.0 (IBM Corporation, Armonk, NY) and the *Stats*, *lme4* and *lmerTest* packages in R Statistical Software version 3.1.3 (R Core Team, 2014). The estimated marginal means are reported by group and time-point for the linear mixed model analyses. Effect sizes were calculated in the linear regression models using partial eta squared ( $h_p^2$ ) and interpreted according to Cohen's guidelines (0.01 = small, 0.06 = medium, 0.14 = large).<sup>19</sup>

## RESULTS

Of 34 eligible children with useable DTI data, 14 were in the CWMT group (13 with an MRI at both T0 and T1) and 20 in the non-training group (18 with an MRI at both T0 and T1) (please refer to Supplemental Figure 1 for the CONSORT flow diagram). Demographic and clinical characteristics did not differ between the CWMT group and the non-training group (Table 1). There were no differences in global white matter microstructure or white matter microstructure on any of the tracts at baseline between the two groups (data not shown).

### White matter microstructure following CWMT

Using a linear mixed model analysis, we found significant group by time interactions with FA in the left SLF significantly higher in the CWMT group compared to the non-training group at T1 (estimated coefficient = .009,  $p = .033$ ), and lower MD in the left SLF in the CWMT group compared to the non-training group at T1 (estimated coefficient = -.010,  $p = .018$ ) (Table 2).

There was a significant group by time interaction with higher global FA in the CWMT group compared to the non-training group at T1 (estimated coefficient = .007,  $p = .015$ ). Additional linear mixed model analyses in the individual tracts showed a significant group by time interaction with higher FA in the right uncinate fasciculus in the CWMT group compared to the non-training group at T1 (estimated coefficient = .013,  $p = .029$ ).

**Table 1.** Study population characteristics

Characteristics	All (n = 34)	Control (n = 19)	CWMT (n = 15)	P-value
<b>a) Demographic</b>				
Age (years)	10 ± 2	10 ± 2	10 ± 1	.821
Gender				.728
Male	21 (62%)	10 (67%)	11 (62%)	
Handedness				
Right	28 (82%)	16 (84%)	12 (80%)	.749
Ethnicity				.355
Dutch	29 (85%)	15 (79%)	14 (93%)	
Maternal education level <sup>a</sup>				.242
Low	5 (15%)	2 (11%)	3 (20%)	
Moderate	11 (32%)	5 (26%)	6 (40%)	
High	18 (53%)	12 (63%)	6 (40%)	
Type of education child				.228
Regular	23 (68%)	13 (68%)	10 (67%)	
Regular with help	9 (26%)	6 (32%)	3 (20%)	
Special education	2 (6%)	0 (0%)	2 (13%)	
IQ	101 ± 12	100 ± 12	102 ± 12	.576
<b>b) Clinical</b>				
Birthweight (kilograms)	3.5 (3.2-2.8)	3.5 (3.3-3.8)	3.4 (3.0-4.0)	.650
Gestational age (weeks)	40 (39-41)	40 (40-41)	40 (40-42)	.483
Mechanical vent. (days)	10 (8-16)	11 (8-16)	10 (9-16)	.762
Chronic lung disease <sup>b</sup>	3 (9%)	2 (11%)	1 (8%)	.787
Abnormal CUS <sup>c</sup>	3 (9%)	2 (12%)	1 (9%)	.823
CDH-non-ECMO	11 (32%)	5 (26%)	6 (40%)	.646
ECMO treatment <sup>d</sup>	23 (68%)	14 (74%)	9 (60%)	.475
Type of ECMO				.176
VA	15 (65%)	8 (57%)	7 (78%)	
VV	7 (30%)	6 (43%)	1 (11%)	
VV conversion to VA	1 (4%)	0 (0%)	1 (22%)	
Age start ECMO (days)	1 (1-2)	2 (1-4)	1 (1-2)	.557
Hours on ECMO	109 (85-180)	114 (84-185)	104 (84-161)	.831

N (%), mean ± SD or median (interquartile range) is reported where appropriate. Dutch refers to children with two native Dutch parents. <sup>a</sup>Based on the highest level of education completed by the mother(38). <sup>b</sup>Chronic lung disease defined as oxygen dependency at 28 days of life<sup>29</sup>. <sup>c</sup>Abnormal CUS: hemorrhagic infarct posterior cerebral artery (n=1), focal densities thalami (n=2). <sup>d</sup>Diagnoses underlying ECMO treatment in the neonatal period were congenital diaphragmatic hernia (n=2), meconium aspiration syndrome (n=17), persistent pulmonary hypertension of the newborn (n = 2), infant respiratory distress syndrome (n = 1), and cardiac anomaly (n=1). Abbreviations: CWMT, Cogmed Working Memory Training; IQ, Intelligence Quotient; CUS, cranial ultrasound; CDH, congenital diaphragmatic hernia; ECMO, extracorporeal membrane oxygenation; VA, venoarterial; VV, venovenous.

**Table 2.** FA and MD group differences in white matter tracts immediately after CWMT

Tract	Hemisphere	Mean FA T1 Non-training	Mean FA T1 CWMT	$p$	$p_{FDR}$	Mean MD T1 Non-training	Mean MD T1 CWMT	$p$
SLF	Left	<b>.390 (.01)</b>	<b>.396 (.01)</b>	<b>.033</b>		<b>.781 (.01)</b>	<b>.770 (.01)</b>	<b>.018</b>
	Right	.387 (.01)	.392 (.01)	.250		.783 (.01)	.762 (.01)	.183
Global	-	<b>.401 (.01)</b>	<b>.406 (.01)</b>	<b>.015</b>		.811 (.01)	.800 (.01)	.055
UNC	Left	.368 (.01)	.381 (.01)	.119	.298			
	Right	.378 (.01)	.392 (.01)	.029	.173			
IFO	Left	.442 (.01)	.451 (.01)	.296	.360			
	Right	.438 (.01)	.447 (.01)	.052	.173			
ILF	Left	.423 (.01)	.424 (.01)	.201	.337			
	Right	.427 (.01)	.429 (.01)	.202	.337			
CB	Left	.382 (.01)	.396 (.01)	.037	.173			
	Right	.351 (.01)	.347 (.01)	.324	.360			
PHC	Left	.276 (.01)	.286 (.01)	.296	.360			
	Right	.295 (.01)	.293 (.01)	.910	.910			

Group\*time-point interaction terms of the linear mixed model analyses showing differences in white matter microstructure between children in the CWMT group ( $n = 14$ ) and non-training group ( $n = 20$ ) directly after the intervention. Mean weighted average FA (SD) is given for each tract per group. Results are significant at  $p$ -value  $< .05$ . The FDR-correction<sup>18</sup> was applied once for the set of additional analyses on the individual white matter tracts (i.e. once for 10 tests).  $P_{FDR} < .05$  was considered statistically significant. Abbreviations: FA, fractional anisotropy; MD, mean diffusivity; UNC, uncinate fasciculus; ILF, inferior longitudinal fasciculus; IFO, inferior fronto-occipital fasciculus; SLF, superior longitudinal fasciculus; CB, cingulum bundle; PHC, parahippocampal cingulum bundle.

However, this finding did not survive the correction for multiple testing ( $p_{FDR} = .173$ ). Furthermore, a significant group by time interaction was found with higher FA in the left cingulum bundle in the CWMT group compared to the non-training group at T1 (estimated coefficient = .019,  $p = .037$ ), but this finding did not remain significant after correcting for multiple testing either ( $p_{FDR} = .173$ )(Table 2).

Global MD did not significantly change following CWMT (estimated coefficient = -.007,  $p = .055$ )(Table 2).

### White matter microstructure and neuropsychological improvement following CWMT

Children in the CWMT group who improved with at least 1 SD on verbal working-memory from T0 to T1 had significantly higher FA in the left SLF at T1 ( $n = 6$ ; FA left SLF at T1 =  $.408 \pm .01$ ) compared to children that did not show this improvement after CWMT ( $n = 6$ ; FA left SLF at T1 =  $.384 \pm .02$ ),  $F(1, 12) = 6.22$ ,  $p = .041$ ,  $h_p^2 = .47$  (Figure 2). This association was not found in the non-training group where two children improved with at least 1 SD from T0 to T1 ( $p = .175$ ), indicating that the association between the increase in FA in the left SLF and improvement in verbal working-memory is related to CWMT.

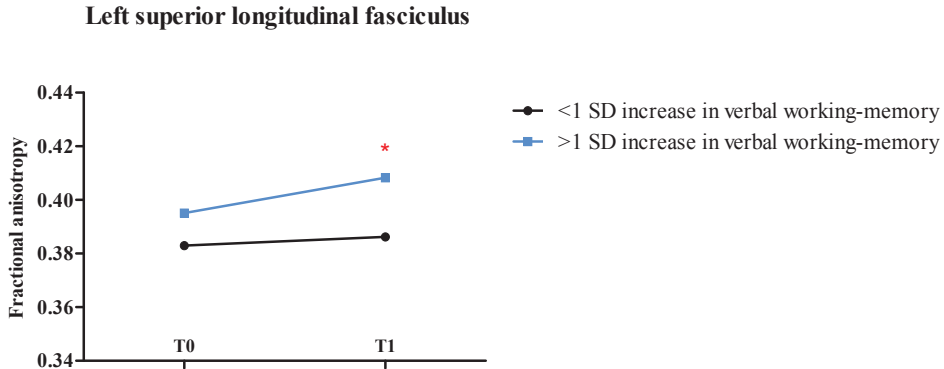


**Figure 2.** Associations between cognitive improvement and changes in white matter microstructure following CWMT

Results from univariate linear regression analyses showing a significant association between an improvement of >1 SD on verbal working-memory and an increase in fractional anisotropy in the SLF after CWMT. Children who improved with at least 1 SD on verbal working-memory ( $n=6$ ) after CWMT, had significantly higher FA in the left SLF at T1 than children that did not show this improvement ( $n=6$ ). \*Indicates a significant association at  $p < .05$ . Abbreviations: CWMT, Cogmed Working-Memory Training.

Significant improvements in visuospatial working-memory or visuospatial memory delayed recall found after CWMT were not associated with the training-induced changes in white matter microstructure in the CWMT group.

## DISCUSSION

In this single-blind randomized controlled trial, we found significant white matter microstructural changes in school-age survivors of neonatal ECMO and/or CDH who were trained with CWMT compared to non-trained survivors. We found both global and specific changes in white matter microstructure immediately post-intervention in the CWMT group compared to the non-training group. Specific changes in FA in the left SLF were associated with better verbal working-memory after CWMT. These findings demonstrate that neurobiological plasticity exists in survivors of neonatal critical illness despite significant alterations found in white matter microstructure in these children compared to healthy controls.<sup>3,5</sup>

Our findings of specific changes in the SLF, a white matter tract connecting the frontal and parietal cortices<sup>9</sup>, following CWMT confirm previous findings of changes in connectivity in frontoparietal regions following working-memory training in healthy school-age children (8-11 years) as well as in childhood cancer survivors (12 years).<sup>20,21</sup> Although most studies have focused on brain *activity* using fMRI and/or were performed in adults, the frontoparietal network has been consistently shown to be affected by working-

memory training.<sup>22-24</sup> Furthermore, we found that the training-induced changes in the left SLF were significantly associated with improvements in verbal working-memory. Predominantly left hemispheric alterations have been previously found following neonatal ECMO<sup>5</sup>, which have been suggested to be due to right internal jugular vein cannulation in neonatal ECMO patients.<sup>25</sup> Because of this, there may be more room for improvement in the left hemisphere, which could explain the training-induced changes in the left hemisphere only. However, we have previously shown that, although more significant alterations were found in the left hemisphere, right-hemispheric alterations were found in these children compared to healthy children as well<sup>3</sup>, making this clarification unlikely. The majority of children in our cohort was right handed (80%) and right-handedness is generally associated with left-hemispheric dominance for language.<sup>26</sup> This therefore may also explain the association between verbal working-memory improvements and the left-sided changes in white matter microstructure. These results confirm previous findings that have shown that working-memory functioning is lateralized, i.e. verbal working-memory corresponds with the left hemisphere and visuospatial working-memory with the right hemisphere.<sup>16,27</sup> However, children in the CWMT group improved significantly on visuospatial working-memory (chapter 7), yet we did not find any changes in the right SLF. In previous neuroimaging studies following CWMT in children as well as adults, both right-lateralized and left-lateralized changes in the frontal and parietal cortices have been demonstrated.<sup>9,21</sup> These contrasting findings may be due to the type of image acquisition and analysis employed, such as region-of-interest versus whole-brain analyses, making it difficult to draw definitive conclusions.

In addition to changes in the left SLF, we found that global FA increased in the CWMT compared to the non-training group from T0 to T1. In the majority of the white matter tracts assessed, FA increased following CWMT. This global change may be due to the relatively high plasticity of the child's brain.<sup>10</sup> Increased FA may indicate enhanced orchestration in communication between neural circuits, which, in turn, may lead to enhanced cognitive functioning.<sup>8</sup> However, these global changes were not associated with any cognitive improvements following CWMT. In the same cohort, we previously showed an association between lower global FA and sustained attention deficits, a domain consistently found to be impaired following neonatal ECMO and/or CDH.<sup>3</sup> However, we did not find any direct relationships between the changes in global FA and sustained attention following CWMT. Future research is needed to better understand the clinical relevance of changes in global white matter microstructure following CWMT in children.

We have previously shown improvements in long-term visuospatial memory both immediately and one year after CWMT in this cohort (chapter 7). These cognitive improvements may be due to changes in brain activity or connectivity that were not detectable using DTI.<sup>9</sup> However, in the same cohort, we previously showed that impaired delayed

visuospatial memory was specifically associated with increased MD in the parahippocampal part of the cingulum.<sup>3</sup> A previous study using DTI in adults following CWMT did find training-induced changes in the parahippocampal cingulum.<sup>9</sup> In our cohort, the improvements in delayed visuospatial memory were most apparent one year post-intervention (chapter 7). Potential changes in the parahippocampal and temporal brain regions therefore may not have been detectable immediately following CWMT. In line with this, a recent study in a population-based cohort of school-age children (6-10 years) has shown downstream effects of behavior on the brain instead of the commonly assumed direction of brain shaping behavior.<sup>28</sup> Such a downstream mechanism may explain why we see cognitive improvements immediately following CWMT without corresponding changes in the brain. Unfortunately, this remains speculative as no MRI was made after one year. Future studies conducting multimodal neuroimaging both immediately and longitudinally over the course of the year post-intervention are needed to better understand neuroplasticity following working-memory training.

This is the first study to assess and demonstrate neuroplasticity following CWMT in neonatal ECMO and/or CDH survivors. Despite this, our study has some limitations. First, our small sample size limits the interpretability of our findings, in particular the analyses on associations between brain changes and cognitive improvement in the CWMT group. However, since the association between increased FA in the SLF and improved verbal working-memory had a large effect size (0.47)<sup>19</sup>, coupled with prior literature supporting this link<sup>9,23</sup>, we regard this to be a reliable finding. Second, we used a non-active control group for ethical considerations against subjecting children to an intensive training without potential benefits, which limits our ability to attribute our findings to the specific characteristics of the CWMT training. However, neuroplasticity has been demonstrated following working-memory training even when compared to a non-adaptive training program.<sup>9,20</sup> Third, we were not able to conduct an MRI exam one year post-intervention, limiting our understanding of neuroplasticity following CWMT. Future studies that combine neuroimaging and neuropsychological assessment at multiple time points following CWMT are needed. Lastly, the indices extracted using DTI are not specific to any white matter property and therefore specific biological changes may be missed. In the future, studies using more sensitive neuroimaging techniques, such as MRI with higher magnetic field strength (e.g. 7 Tesla), will further increase our understanding of neuroplasticity following cognitive training.

## CONCLUSION

Our findings demonstrate both global and specific changes in white matter microstructure immediately after CWMT in school-age survivors of neonatal ECMO and/or CDH

compared to non-trained survivors. Specific changes in FA in the left SLF were associated with better verbal working-memory after CWMT. These results suggest that white matter microstructure and associated cognitive outcomes are malleable in these children. Future studies on the effectiveness of cognitive interventions need to include follow-up assessments both immediately and one year after the training to further increase our understanding of neuroplasticity following neonatal critical illness.

## REFERENCES

1. Leeuwen L, Schiller RM, Rietman AB, van Rosmalen J, Wildschut ED, Houmes RJM, et al. Risk Factors of Impaired Neuropsychologic Outcome in School-Aged Survivors of Neonatal Critical Illness. *Crit Care Med*. 2017;46(3):401-410.
2. Madderom MJ, Schiller RM, Gischler SJ, van Heijst AF, Tibboel D, Aarsen FK, et al. Growing Up After Critical Illness: Verbal, Visual-Spatial, and Working Memory Problems in Neonatal Extracorporeal Membrane Oxygenation Survivors. *Crit Care Med*. 2016;44(6):1182-1190.
3. Schiller RM, IJsselstijn H, Madderom MJ, Rietman AB, Smits M, van Heijst AFJ, et al. Neurobiologic Correlates of Attention and Memory Deficits Following Critical Illness in Early Life. *Crit Care Med*. 2017;45(10):1742-1750.
4. Cooper JM, Gadian DG, Jentschke S, Goldman A, Munoz M, Pitts G, et al. Neonatal hypoxia, hippocampal atrophy, and memory impairment: evidence of a causal sequence. *Cereb Cortex*. 2015;25(6):1469-1476.
5. Schiller RM, van den Bosch GE, Muetzel RL, Smits M, Dudink J, Tibboel D, et al. Neonatal critical illness and development: white matter and hippocampus alterations in school-age neonatal extracorporeal membrane oxygenation survivors. *Dev Med Child Neurol*. 2017;59(3):304-310.
6. Klingberg T, Forssberg H, Westerberg H. Training of working memory in children with ADHD. *J Clin Exp Neuropsychol*. 2002;24(6):781-791.
7. Caeyenberghs K, Metzler-Baddeley C, Foley S, Jones DK. Dynamics of the Human Structural Connectome Underlying Working Memory Training. *J Neurosci*. 2016;36(14):4056-4066.
8. Takeuchi H, Sekiguchi A, Taki Y, Yokoyama S, Yomogida Y, Komuro N, et al. Training of working memory impacts structural connectivity. *J Neurosci*. 2010;30(9):3297-3303.
9. Metzler-Baddeley C, Foley S, de Santis S, Charron C, Hampshire A, Caeyenberghs K, et al. Dynamics of White Matter Plasticity Underlying Working Memory Training: Multimodal Evidence from Diffusion MRI and Relaxometry. *J Cogn Neurosci*. 2017;29(9):1509-1520.
10. Kolb B, Mychasiuk R, Muhammad A, Gibb R. Brain plasticity in the developing brain. *Prog Brain Res*. 2013;207:35-64.
11. Lezak MD, Howieson DB, Loring DW. *Neuropsychological assessment, 4th ed*. Oxford: Oxford University Press; 2004.
12. White T, El Marroun H, Nijs I, Schmidt M, van der Lugt A, Wielopolki PA, et al. Pediatric population-based neuroimaging and the Generation R Study: the intersection of developmental neuroscience and epidemiology. *Eur J Epidemiol*. 2013;28(1):99-111.
13. de Groot M, Ikram MA, Akoudad S, Krestin GP, Hofman A, van der Lugt A, et al. Tract specific white matter degeneration in aging: the Rotterdam Study. *Alzheimers Dement*. 2015;11(3):321-330.
14. Muetzel RL, Mous SE, van der Ende J, Blanken LM, van der Lugt A, Jaddoe VW, et al. White matter integrity and cognitive performance in school-age children: A population based neuroimaging study. *Neuroimage*. 2015;119:119-128.
15. Schmithorst VJ, Wilke M, Dardzinski BJ, Holland SK. Cognitive functions correlate with white matter architecture in a normal pediatric population: a diffusion tensor MRI study. *Hum Brain Mapp*. 2005;26(2):139-147.
16. Ocklenburg S, Hirnstein M, Beste C, Gunturkun O. Lateralization and cognitive systems. *Front Psychol*. 2014;5:1143.
17. Lebel C, Walker L, Leemans A, Phillips L, Beaulieu C. Microstructural maturation of the human brain from childhood to adulthood. *Neuroimage*. 2008;40(3):1044-1055.

18. Benjamini Y, Hochberg Y. Controlling the False Discovery Rate - a Practical and Powerful Approach to Multiple Testing. *J Roy Stat Soc B Met.* 1995;57(1):289-300.
19. Cohen J. *Statistical power analysis for the behavioral sciences, 2nd ed* Hillsdale, NJ: Lawrence Erlbaum Associates; 1988.
20. Astle DE, Barnes JJ, Baker K, Colclough GL, Woolrich MW. Cognitive training enhances intrinsic brain connectivity in childhood. *J Neurosci.* 2015;35(16):6277-6283.
21. Conklin HM, Ogg RJ, Ashford JM, Scoggins MA, Zou P, Clark KN, et al. Computerized Cognitive Training for Amelioration of Cognitive Late Effects Among Childhood Cancer Survivors: A Randomized Controlled Trial. *J Clin Oncol.* 2015;33(33):3894-3902.
22. Klingberg T. Training and plasticity of working memory. *Trends Cogn Sci.* 2010;14(7):317 - -324.
23. Olesen PJ, Westerberg H, Klingberg T. Increased prefrontal and parietal activity after training of working memory. *Nat Neurosci.* 2004;7(1):75-79.
24. Jolles DD, van Buchem MA, Crone EA, Rombouts SA. Functional brain connectivity at rest changes after working memory training. *Hum Brain Mapp.* 2013;34(2):396-406.
25. Raets MM, Dudink J, IJsselstijn H, van Heijst AF, Lequin MH, Houmes RJ, et al. Brain injury associated with neonatal extracorporeal membrane oxygenation in the Netherlands: a nationwide evaluation spanning two decades. *Pediatr Crit Care Med.* 2013;14(9):884-892.
26. Szaflarski JP, Rajagopal A, Altaye M, Byars AW, Jacola L, Schmithorst VJ, et al. Left handedness and language lateralization in children. *Brain Res.* 2012;1433:85-97.
27. Nagel BJ, Herting MM, Maxwell EC, Bruno R, Fair D. Hemispheric lateralization of verbal and spatial working memory during adolescence. *Brain Cogn.* 2013;82(1):58-68.
28. Muetzel RL, Blanken LME, van der Ende J, El Marroun H, Shaw P, Sudre G, et al. Tracking Brain Development and Dimensional Psychiatric Symptoms in Children: A Longitudinal Population Based Neuroimaging Study. *Am J Psychiatry.* 2017:appiajp201716070813.
29. Jobe AH, Bancalari E. Bronchopulmonary dysplasia. *Am J Respir Crit Care Med.* 2001;163(7):1723-1729.

## SUPPLEMENTARY MATERIAL

### Supplemental File 1. Descriptions of the neuropsychological tests.

#### *Intelligence*

##### Wechsler Intelligence Scale for Children (WISC-III-NL)

A short-form with two subtests, Block Design and Vocabulary, of the WISC-III-NL were used to assess general intelligence.<sup>1</sup> The WISC-III-NL has been shown to have good reliability and validity.<sup>2</sup> A normalized population mean of 100 with a standard deviation of 15 is used.<sup>2</sup>

#### *Verbal working-memory*

##### WISC-III-NL – subtest Digit Span

The Digit Span consists of random number sequences that increase in length and that the examiner reads aloud at the rate of 1 number per second. The child has to reproduce these numbers in the same order. Next, the sequences must be recalled backwards (3-5-7 becomes 7-5-3). The first part of the test measures short-term auditory memory and short-term retention capacity. The second part measures auditory working memory.<sup>2</sup>

#### *Visuospatial working-memory*

##### Wechsler Nonverbal Scale of Ability (WNV) – subtest Spatial Span

The Spatial Span requires the child to touch a group of blocks arranged on a board in a non-systematic manner in the same and reverse order as demonstrated by the examiner. The first part of the test measures short-term visuospatial memory and short-term retention capacity. The second part measures visuospatial working-memory.<sup>3</sup>

#### *Verbal memory*

##### Rey Auditory Verbal Learning Test (RAVLT)

The RAVLT consists of five presentations with recall of a 15-word list, a sixth recall trial after 30 minutes, and a seventh recognition trial. This test measures memory span, short- and long term verbal memory, verbal recognition, and learning curve. It can be administered to children and adults in the age range 6-89 years.<sup>4,5</sup>

#### *Visuospatial memory and visuospatial processing*

##### Rey Complex Figure Test (RCFT)

The RCFT consists of three trials. First the child has to copy a complex figure (Copy). Then after 3 and after 30 minutes the figure must be drawn from memory (Recall). Next, different figures are shown and the child has to indicate whether these figures were in the original figure (Recognition). This test measures visual integration, short- and long-term

visual-spatial memory, and visual-spatial recognition. It can be completed by children and adults in the age range 6-89 years.<sup>6,7</sup>

### **Attention**

#### Dot Cancellation Test

This paper-and-pencil test measures sustained attention and concentration in terms of speed. It consists of a paper on which figures made of three, four or five dots are displayed in 33 rows. The child is instructed to mark all figures with four dots, as precisely and as fast as they can.<sup>8</sup>

#### Stroop Colour Word Test (Stroop)

The Stroop consists of three trials: in the first trial (Stroop 1) the subject must read colour names, in the second trial (Stroop 2) name printed colours, and in the third trial (Stroop 3) name printed colours not denoted by the colour name. The test can be administered to children and adults in the age range 8-65 years. Selective attention is measured with this test, using the difference score between Stroop 2 and Stroop 3.<sup>9,10</sup>

#### Trail Making Test (TMT)

This paper and pencil test consists of two parts. In the first part (part A), the subject must draw lines to consecutively connect numbered circles on a sheet. In the second part (part B), the subject must consecutively but alternately connect numbered and lettered circles on another worksheet. The aim of the test is to finish each part as quickly as possible. The test can be administered to children and adults in the age range 6-89 years. This test measures visual conceptual and visuomotor tracking as well as divided attention.<sup>9,10</sup>

### **Executive functioning**

#### Key Search of the Behavioural Assessment of the Dysexecutive Syndrome (BADS-C-NL)

A test of strategy formation. The child is asked to demonstrate how they would search a field for a set of lost keys and their strategy is scored according to its efficiency and functionality.<sup>11</sup>

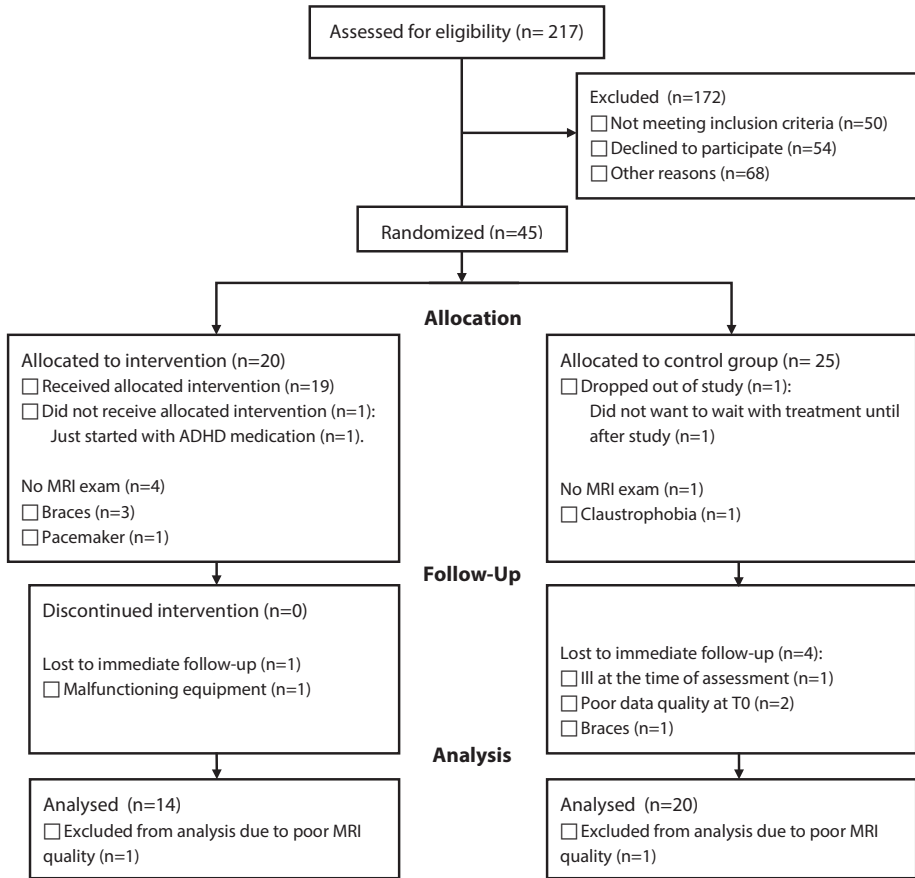
#### Modified Six Elements of the BADS-C-NL

The child is asked to work on six different tasks for which they have five minutes. The child needs to make sure that by the end of the five minutes, all six of the tasks have been done and the child has done as much as possible of each task. This is a test of planning, task scheduling and performance monitoring.<sup>11</sup>

We used Dutch versions of all tests.

## REFERENCES

1. Kaufman AS, Kaufman JC, Balgopal R, McLean JE. Comparison of three WISC-III short forms: Weighing psychometric, clinical, and practical factors. *J Clin Child Psychol.* 1996;25(1):97-105.
2. Kort W, Compaan EL. *WISC NL III. Handleiding.* NIP Dienstencentrum 1999.
3. Wechsler D, Naglieri JA. *Wechsler Nonverbal Scale of Ability* San Antonio, TX: Pearson; 2006.
4. van den Burg W, Kingma A. Performance of 225 Dutch school children on Rey's Auditory Verbal Learning Test (AVLT): parallel test-retest reliabilities with an interval of 3 months and normative data. *Arch Clin Neuropsychol.* 1999;14(6):545-559.
5. Schmidt M. *Rey Auditory and Verbal Learning Test: a handbook.* Los Angeles, CA: Western Psychological Services; 1996.
6. Meyers JE, Meyers, K.R. *Rey Complex Figure Test and Recognition Trial Supplemental Norms for Children and Adolescents.* Lutz: Psychological Assessment Resources; 1996.
7. Lezak MD, Howieson, D.B., Loring, D.W. *Neuropsychological Assessment, 4th ed.* Oxford: Oxford University Press; 2004.
8. Vos P. *Bourdon-Vos. Handleiding (manual dot cancellation test).* Lisse: Swets en Zeitlinger; 1992.
9. Lezak MD, Howieson DB, Loring DW. *Neuropsychological assessment, 4th ed.* Oxford: Oxford University Press; 2004.
10. Schmand B, Houx P, De Koning I. *Dutch norms for Stroop color-word test, Trail making test, Rey auditory verbal-learning test, Verbal fluency, and Story recall of Rivermead behavioural memory test.* Amsterdam: Division Neuropsychology of the Dutch Institute for Psychology; 2003.
11. Emslie H, Wilson FC, Burden V, Nimmo-Smith I, Wilson BA. *Behavioral assessment of the dysexecutive syndrome for children (BADs-C), Dutch version.* Amsterdam Harcourt; 2006.



**Supplemental Figure 1.** CONSORT flow diagram  
 Abbreviations: ADHD, Attention Deficit Hyperactivity Disorder.

## Supplemental File 2. Neuroimaging methods.

### *Image Acquisition*

Prior to neuroimaging, all participants underwent a 30-minute mock scanning session to become familiarized with the MR-environment<sup>1</sup>. Magnetic resonance imaging data were acquired on a 3 Tesla GE MR-750W system using an 8 channel receive-only head coil (General Electric, Milwaukee, WI). In order to support the participant's head and minimize head motion, cushions were placed on both sides of the child's head inside of the head coil. Participants were able to watch a movie during the scans. MRI-compatible headphones were used to reduce the scanner noise and allow participants to listen to the movie's audio track. Communication with the MR operator was also enabled through the headphones before and after scans. The DTI data were acquired using a single-shot, echo-planar imaging sequence with the following parameters: TR = 12,500 ms, TE = 72 ms, flip angle = 90, matrix = 120 x 120, FOV = 240 mm x 240 mm, slice thickness = 2 mm, number of slices = 65, ASSET acceleration factor = 2. In total, 35 volumes with diffusion weighting ( $b = 900 \text{ s/mm}^2$ ) and 3 volumes without diffusion weighting ( $b = 0 \text{ s/mm}^2$ ) were acquired.

### *MR-Image Preprocessing*

Data were processed using the Functional MRI of the Brain's Software Library (FMRIB, FSL) (2) and the Camino Diffusion MRI Toolkit within Python (version 2.7) and the Neuroimaging in Python Pipelines and Interfaces package (Nipype, version 0.92)<sup>3,4</sup>. First, motion and eddy-current induced artifacts<sup>5</sup> were addressed using the FSL "eddy\_correct" tool<sup>6</sup>. In order to account for the rotations applied to the diffusion data after adjusting for these artifact, the resulting transformation matrices were used to rotate the "B-matrix" gradient direction table<sup>7,8</sup>. The FSL Brain Extraction Tool was used to remove non-brain tissue<sup>9</sup>. In order to minimize the limitations observed with respect to the ordinary least squares fit method<sup>10</sup>, the diffusion tensor was fit using the RESTORE method implemented in Camino<sup>11</sup>. Voxel-wise scalar maps (i.e. FA, MD) were then computed. FA is the degree of directionality of diffusion and ranges from 0 to 1, where a higher FA generally represents a greater coherence of white matter fibers. MD is the rate of diffusion of hydrogen averaged in all directions. Lower MD is suggestive of increased integrity in axonal membranes, packing, or myelin. White matter continues to mature throughout childhood, even into young adulthood, causing FA to increase and MD to decrease. Abnormal brain development typically leads to lower FA and higher MD in white matter tracts<sup>12</sup>.

### *Probabilistic Fiber Tractography*

Fully automated probabilistic fiber tractography was performed using the FSL plugin, "AutoPtx"<sup>13</sup>. Subject-specific, probabilistic representations of multiple white matter fiber

bundles are created with this method using a combination of FSL tools from the Diffusion Toolkit (FDT). The Bayesian Estimation of Diffusion Parameters Obtained using Sampling Techniques (BEDPOSTx), accounting for two fiber orientations at each voxel, was used to estimate diffusion parameters at each voxel<sup>14,15</sup>. Next, for each subject, the FA map was aligned to the FMRIB-58 FA template image with the FSL nonlinear registration tool (FNIRT). The inverse of this nonlinear warp field was computed, and applied to a series of predefined seed, target, exclusion, and termination masks provided by the AutoPtx plugin (<http://fsl.fmrib.ox.ac.uk/fsl/fslwiki/AutoPtx>). The FSL module "ProbtrackX" was then applied to conduct probabilistic fiber tracking using these supplied tract-specific masks (i.e., seed, target, etc.) in the native diffusion image space of each subject<sup>14</sup>. The connectivity distributions resulting from fiber tractography were normalized to a scale from 0 to 1 using the total number of successful seed-to-target attempts, and were subsequently thresholded to remove low-probability voxels likely related to noise. For each tract, the number of samples used for probabilistic tracking, and the probability thresholds applied to the resulting distributions (ILF: 0.005, SLF: 0.001, IFO: 0.01, UNC: 0.01, CB: 0.01, PHC: 0.02), were selected based on previously established values<sup>13</sup>. After thresholding the path distributions, weighted average DTI scalar measures were computed within each tract using the normalized path distributions as the weights. The methods used were based on those described by Muetzel et al<sup>16</sup>.

### *Image Quality Assurance*

Raw DTI image quality was assessed with both a visual inspection and with automated software<sup>16</sup>. For the visual inspection, maps of the sum of squares error (SSE) of the tensor fit were inspected for structured signal that is consistent with motion and other artifacts in the diffusion-weighted images (e.g., attenuated slices in diffusion-weighted images). Furthermore, probabilistic tractography data were inspected visually to ensure images were properly aligned to the template and paths were reconstructed accurately<sup>16</sup>. Datasets determined to be of poor quality were excluded ( $n = 7$ , ~8%).

In addition to this visual inspection, slice-wise signal intensity was examined for attenuation resulting from motion, cardiac pulsation and other artifacts using the automated DTIprep quality control tool (<http://www.nitrc.org/projects/dtprep/>). Four (~5%) additional datasets were excluded based on the DTIprep results, leaving 77 DTI datasets (patients = 23, controls = 54) for analysis.

## REFERENCES

1. White T, El Marroun H, Nijs I, Schmidt M, van der Lugt A, Wielopolski PA, et al. Pediatric population-based neuroimaging and the Generation R Study: the intersection of developmental neuroscience and epidemiology. *Eur J Epidemiol.* 2013;28(1):99-111.

2. Jenkinson M, Beckmann CF, Behrens TE, Woolrich MW, Smith SM. *Fsl. Neuroimage*. 2012;62(2):782-90.
3. Cook PA, Bai, Y, Nedjati-Gilani, S, Seunarine, KK, Hall, MG, Parker, GJ, Alexander, DC. Camino: open-source diffusion-MRI reconstruction and processing. 14th Scientific Meeting of the International Society for Magnetic Resonance in Medicine. Seattle, WA, USA2006. p. 2759.
4. Gorgolewski K, Burns CD, Madison C, Clark D, Halchenko YO, Waskom ML, et al. Nipype: a flexible, lightweight and extensible neuroimaging data processing framework in python. *Front Neuroinform*. 2011;5:13.
5. Haselgrove JC, Moore JR. Correction for distortion of echo-planar images used to calculate the apparent diffusion coefficient. *Magn Reson Med*. 1996;36(6):960-4.
6. Jenkinson M, Smith S. A global optimisation method for robust affine registration of brain images. *Med Image Anal*. 2001;5(2):143-56.
7. Jones DK, Cercignani M. Twenty-five pitfalls in the analysis of diffusion MRI data. *NMR Biomed*. 2010;23(7):803-20.
8. Leemans A, Jones DK. The B-matrix must be rotated when correcting for subject motion in DTI data. *Magn Reson Med*. 2009;61(6):1336-49.
9. Smith SM. Fast robust automated brain extraction. *Hum Brain Mapp*. 2002;17(3):143-55.
10. Veraart J, Sijbers J, Sunaert S, Leemans A, Jeurissen B. Weighted linear least squares estimation of diffusion MRI parameters: strengths, limitations, and pitfalls. *Neuroimage*. 2013;81:335-46.
11. Chang LC, Jones DK, Pierpaoli C. RESTORE: robust estimation of tensors by outlier rejection. *Magn Reson Med*. 2005;53(5):1088-95.
12. Lebel C, Beaulieu C. Longitudinal development of human brain wiring continues from childhood into adulthood. *J Neurosci*. 2011;31(30):10937-47.
13. de Groot M, Ikram MA, Akoudad S, Krestin GP, Hofman A, van der Lugt A, et al. Tract-specific white matter degeneration in aging: the Rotterdam Study. *Alzheimers Dement*. 2015;11(3):321-30.
14. Behrens TE, Berg HJ, Jbabdi S, Rushworth MF, Woolrich MW. Probabilistic diffusion tractography with multiple fibre orientations: What can we gain? *Neuroimage*. 2007;34(1):144-55.
15. Behrens TE, Woolrich MW, Jenkinson M, Johansen-Berg H, Nunes RG, Clare S, et al. Characterization and propagation of uncertainty in diffusion-weighted MR imaging. *Magn Reson Med*. 2003;50(5):1077-88.
16. Muetzel RL, Mous SE, van der Ende J, Blanken LM, van der Lugt A, Jaddoe VW, et al. White matter integrity and cognitive performance in school-age children: A population-based neuroimaging study. *Neuroimage*. 2015;119:119-28.
17. Vogt BA, Finch DM, Olson CR. Functional heterogeneity in cingulate cortex: the anterior executive and posterior evaluative regions. *Cereb Cortex*. 1992;2(6):435-43.
18. van den Bosch GE, H IJsselstijn, van der Lugt A, Tibboel D, van Dijk M, White T. Neuroimaging, Pain Sensitivity, and Neuropsychological Functioning in School-Age Neonatal Extracorporeal Membrane Oxygenation Survivors Exposed to Opioids and Sedatives. *Pediatr Crit Care Med*. 2015;16(7):652-62.